

# Calibration of NOAA16 AVHRR over a desert site using MODIS data

E.F. Vermote<sup>a,\*</sup>, N.Z. Saleous<sup>b</sup>

<sup>a</sup> University of Maryland, Department of geography and NASA GSFC Code 614.5, United States

<sup>b</sup> SAIC and NASA GSFC Code 614.5, United States

Received 24 February 2006; received in revised form 16 June 2006; accepted 27 June 2006

## Abstract

This paper presents a new approach to AVHRR-sensors cross-calibration in the visible to shortwave-infrared spectral domain using an a-priori, well calibrated sensor (MODIS). The approach has been tested over a stable Sahara desert site and was initially applied to compare the absolute calibration coefficients of three different bands of the Terra and Aqua MODIS instruments. The observed agreement was better than 1% for bands 1 (0.67  $\mu\text{m}$ ), 2 (0.87  $\mu\text{m}$ ) and 7 (2.13  $\mu\text{m}$ ). The approach was then applied to cross-calibrate the AVHRR sensor onboard NOAA16. The absolute calibration coefficients derived for bands 1 and 2, using the Terra MODIS as a reference, were compared to the vicarious coefficients derived using the ocean and clouds method [Vermote E.F. and Kaufman Y.J. (1995). Absolute calibration of AVHRR visible and near-infrared channels using ocean and cloud views, *International Journal of Remote Sensing*, 16, 13, 2317–2340.]. The coefficients were consistent within less than 1%. © 2006 Elsevier Inc. All rights reserved.

**Keywords:** Calibration; AVHRR; MODIS

## 1. Introduction

The Advanced Very High Resolution Radiometer (AVHRR) onboard NOAA polar orbiting satellites has acquired over 20 years of global data. This constitutes the longest record of global remotely sensed imagery of the earth surface and is invaluable in land surface and global climate change studies. Unfortunately, AVHRR lacks an onboard calibration capability for its visible to middle infrared bands. To circumvent this shortcoming, a variety of vicarious calibration techniques has been developed; they include the use of an invariant desert target (Heidinger et al., 2002b; Rao & Chen, 1996) and simulated ocean signal (Vermote & Kaufman, 1995). The calibration accuracy achieved by these different approaches does not exceed 5%.

The cross-calibration approach has been used in the past (Teillet et al., 2001) and is particularly attractive with the arrival of well calibrated sensors, equipped with state of the art onboard calibration instrumentation. The Moderate Resolution Imaging Spectroradiometer (MODIS), which acquires global data on a

daily basis, offers an alternative approach by which the accurate calibration is transferred to AVHRR using targets of known reflectance. Heidinger et al. (2002a) proposed a cross-calibration approach using coincident, near nadir, acquisitions of MODIS and AVHRR over Alaska and Siberia.

For our research, we used MODIS data to derive a full spectral and directional parameterization of an invariant desert target, then use this data to predict the AVHRR surface reflectance over the site and perform a cross-calibration.

The MODIS instrument onboard the Earth Observing System's (EOS) Terra platform has been acquiring global data since February 2000. Its solar reflective bands have been calibrated to reflectance units using state of the art onboard calibration system with an absolute accuracy better than 2% (Guenther et al., 2002). The land spectral bands have been carefully selected to avoid major contamination by water vapor which constitutes a major limitation of previous earth remote sensing missions such as AVHRR (Justice et al., 1991). In addition, MODIS has two water vapor absorption bands in the near-infrared spectrum (bands 18 and 19) that enable very accurate retrieval of the integrated amount of water vapor; a measure needed to perform adequate correction of water vapor absorption in the land bands.

\* Corresponding author. 4321 Hartwick Rd, Suite 209, College Park, MD, 20742 USA.

E-mail address: [eric@ltdri.org](mailto:eric@ltdri.org) (E.F. Vermote).

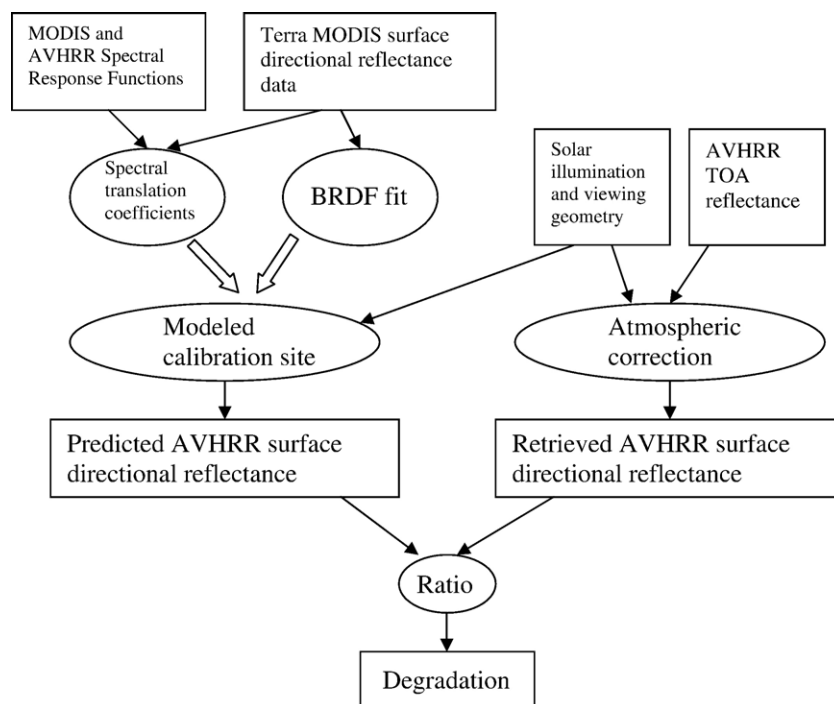


Fig. 1. Block diagram describing the cross-calibration approach.

The cross-calibration approach relies on using Terra MODIS data to fully characterize a stable desert site that serves as an invariant target in the cross-calibration of the AVHRR reflectance bands. We use 2 years of Terra MODIS data to fit a BRDF (Bidirectional Reflectance Distribution Function) model to characterize the directional behavior of the site. Terra MODIS data are also used to derive spectral translation equations to account for the spectral differences between MODIS and AVHRR

bands. More details about the site spectral and directional characterization are presented in Section 2. Fig. 1 shows a block diagram summarizing the different steps of the cross-calibration approach. The site BRDF parameterization is used to predict the surface reflectance for any set of solar illumination and viewing geometries. The spectral translation equations are used to adjust the predicted reflectance to AVHRR spectral bands. The ratio of the observed surface reflectance to the modeled reflectance is then used to predict the sensor degradation and offer a calibration adjustment coefficient.

To assess the performance of this cross-calibration approach, we use it to transfer the calibration to Aqua MODIS reflectance bands and compare the results to the in-flight calibration performed by the MODIS Characterization Support Team (MCST) using the onboard solar diffuser. The results are presented in Section 3 and show excellent agreement between the two methods.

In order to apply this technique to AVHRR, we start by performing an atmospheric correction of the data. Since AVHRR does not have water vapor absorption bands, we establish a relation to derive the water vapor content from bands 4 and 5 (11 and 12  $\mu\text{m}$ , respectively) using a split window technique. The approach and results are presented in Section 4. Finally, we compared the results of the cross-calibration approach to those obtained using the ocean and clouds method (Vermote & Kaufman, 1995).

## 2. Calibration site characterization using Terra MODIS data

For this study, we selected a stable Saharan desert site southwest of the Tibesti Mountains in Niger. The site, indicated by the red square on the MODIS July 13, 2002 true color image shown in Fig. 2, measures about 20 km  $\times$  20 km and is centered at 21.5°North and 14.4°East.



Fig. 2. Location of the 20 km by 20 km calibration site (centered on the red square) The image represents an area of 1000 km by 1000 km.

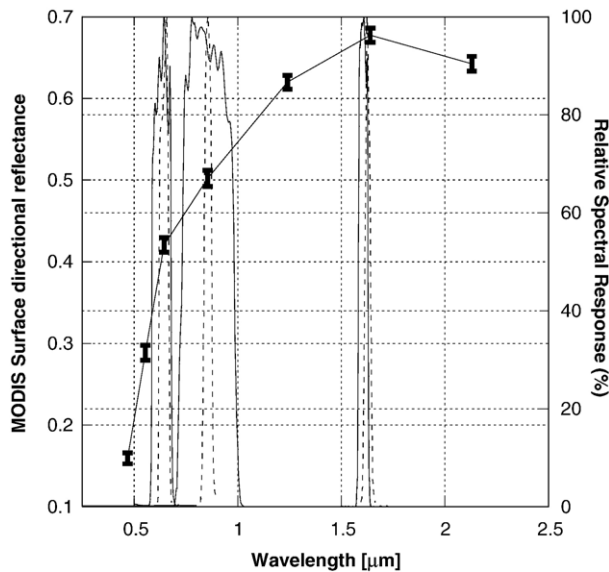


Fig. 3. Surface directional reflectance observed for land bands (1–7) over the calibration site on July 13, 2002 by the MODIS-Terra instrument. The error bars represent the standard deviation. The relative spectral responses of the NOAA16 AVHRR bands 1, 2 and 3 (solid line) and MODIS bands 1, 2 and 6 (dashed lines) are also plotted.

To use this site as a cross-calibration target, we began by deriving an accurate characterization, including spectral and directional properties. To determine the spectral behavior, we plotted the average Terra MODIS retrieved reflectance over the site as a function of the MODIS central wavelength. Fig. 3 shows a plot of the MODIS surface reflectance in all land bands (bands 1 through 7) for data acquired on July 13, 2002. Due to the spectral difference between AVHRR and the corresponding MODIS bands, we expect to observe differences in the AVHRR and MODIS reflectance. Assuming that the spectral behavior of the site is stable in time, and knowing the spectral response functions for AVHRR and MODIS bands, we derived translation equations to compute AVHRR reflectance over the site as a function of MODIS reflectance. Fig. 3 also shows the spectral response functions for AVHRR bands 1 (0.645  $\mu\text{m}$ ), 2 (0.865  $\mu\text{m}$ ) and 3 (1.6  $\mu\text{m}$ ), and MODIS bands 1 (0.645  $\mu\text{m}$ ), 2 (0.865  $\mu\text{m}$ ) and 6 (1.65  $\mu\text{m}$ ). Given the spectral behavior of the site, and the spectral response functions of both instruments, we derived a linear translation equation of the form  $\rho_{\text{avhrr},i} = a_i \rho_{\text{modis},j}$  where  $i$

Table 1  
Calibration site characterization coefficients

Spectral translation coefficients			
	AVHRR 1 (0.645 $\mu\text{m}$ )	AVHRR 2 (0.865 $\mu\text{m}$ )	AVHRR 3 (1.6 $\mu\text{m}$ )
$a_i$	0.952	0.988	0.994
Calibration site BRDF model parameters			
	MODIS 1 (0.645 $\mu\text{m}$ )	MODIS 2 (0.865 $\mu\text{m}$ )	MODIS 6 (1.6 $\mu\text{m}$ )
Isotropic	0.39951	0.48252	0.66633
RosThick	0.17318	0.16268	0.12016
LiSparseR	-0.00931	-0.00671	0.00424

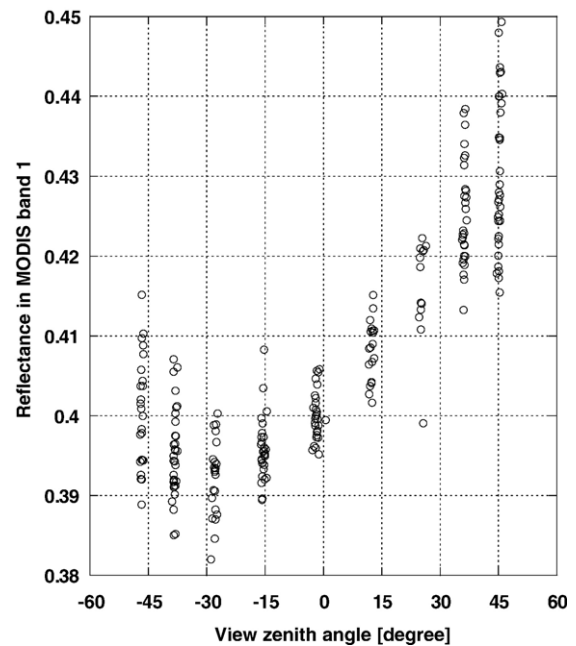


Fig. 4. Variation of the surface directional reflectance in MODIS band 1 as a function of view zenith angle during the two years period used to characterize the desert site.

represents AVHRR band and  $j$  the corresponding MODIS band. The coefficients for  $a_i$  are included in Table 1.

To determine the directional reflectance behavior of the site, we used the operational MODIS Bidirectional Reflectance Distribution Function (BRDF) algorithm. This relies on a kernel-driven linear BRDF model, defined as a weighted sum of an isotropic parameter, a RossThick and a LiSparseReciprocal kernel (Schaaf et al., 2002). To determine the coefficients describing the calibration site, we used approximately 2 years of Terra MODIS data where the instrument configuration was stable (from November 2, 2000 to September, 7 2002). In addition to the operational cloud screening, an additional cloud

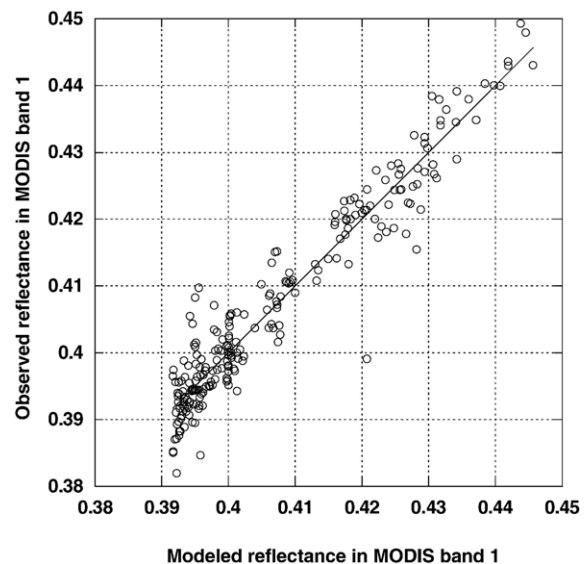


Fig. 5. Comparison of the modeled and the retrieved surface directional reflectance in band 1 using the MODIS BRDF model.

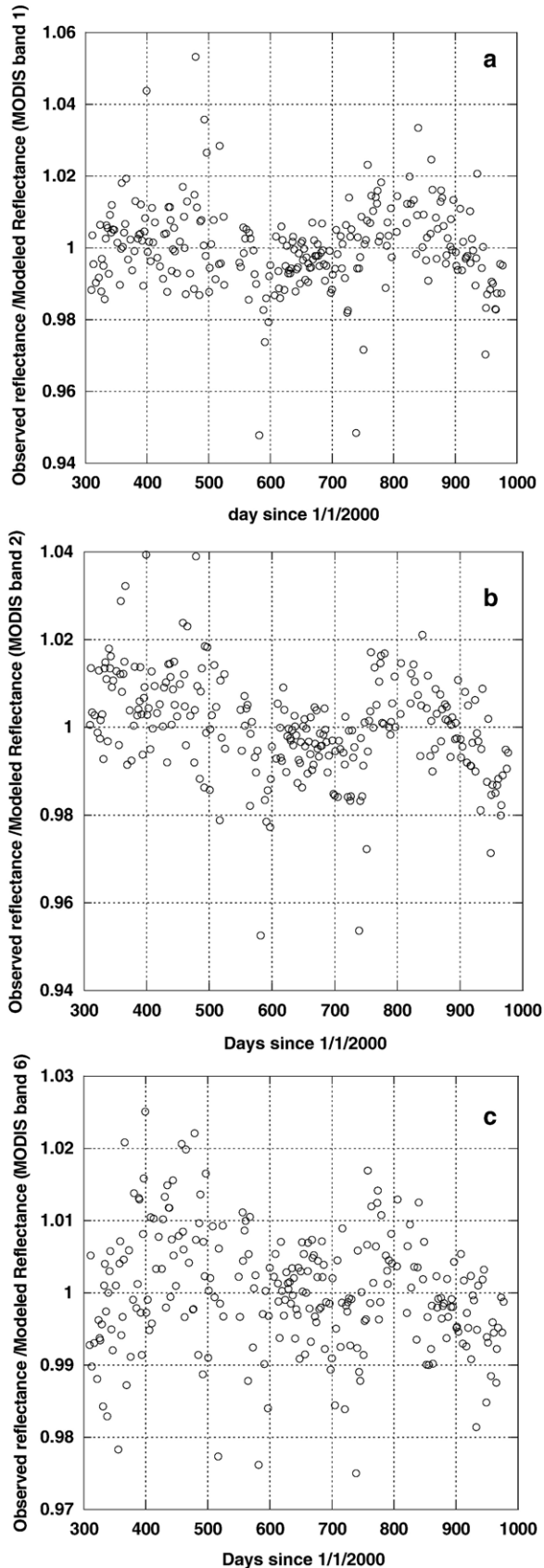


Fig. 6. (a) ratio between the observed and the modeled surface directional reflectance in band 1 during the site characterization period (November 2, 2000 to September 7, 2002). (b) Same as in (a) but for band 2. (c) Same as in (a) but for band 6.

filtering based on the standard deviation of MODIS band 7 reflectance over the site is applied. This rigorous cloud screening removes subpixel cloud contamination and ensures that only clear observations are retained. Observations that fall within  $15^\circ$  of backscattering conditions are also excluded to avoid the hot-spot (Vermote & Roy, 2002), as it is not included in the MODIS kernel BRDF models (Schaaf et al., 2002). Since it becomes difficult to find coincident AVHRR and MODIS footprints for view zenith angles greater than  $50^\circ$ , due to variation in pixel geometry, we exclude these observations in our study. A plot of the MODIS surface reflectance, as a function of the view zenith angle for band 1 ( $0.645 \mu\text{m}$ ), is shown in Fig. 4. The sign of the view zenith angle was arbitrarily set to negative if the relative azimuth was between  $0$  and  $90^\circ$ , and to positive if the relative azimuth was between  $90^\circ$  and  $180^\circ$ . As it can be seen on Fig. 4, the reflectance, though also varying with relative azimuth and solar zenith angle for each class of view zenith angle, shows systematic variation that is due to directional effects. These directional effects, although relatively small ( $\sim 20\%$ ) compared to the effects observed over vegetation, still need to be taken into account before the site can be used as an invariant target for vicarious calibration. The BRDF model coefficients derived using the 2 years of Terra MODIS data are listed in Table 1. They are used to compute the site's modeled surface reflectance in MODIS land bands for the same geometric conditions as the data used in the study. Fig. 5 shows a plot of the modeled reflectance versus the retrieved reflectance for MODIS band 1. As it can be seen, the MODIS BRDF model can explain the major part of the variability in the data set. The standard deviation between the observed and the modeled reflectance is  $4.2 \cdot 10^{-3}$  in reflectance unit, which roughly corresponds to a relative variation of 1%.

In order to verify the validity of the site parameterization for the purpose of cross-calibration, we plot the ratio between the observed and the modeled reflectance for MODIS bands 1, 2 and 6 as a function of time for the period November 2, 2000 to September 7, 2002 (Fig. 6a–c). These figures show that the BRDF model used accurately represents the site and allows predicting the surface reflectance for different geometric conditions. The majority of points (98.5% for band 1, 94.2% for band 2 and 96.9% for band 6) fall between 0.98 and 1.02 (error of 2%).

### 3. Verification of the approach using Aqua MODIS data

To assess the performance of the proposed cross-calibration approach, we applied it to cross-calibrate MODIS reflectance bands on Aqua, using the site characterization derived from Terra. The results were then compared to those derived from the onboard calibration.

To apply the cross-calibration approach to Aqua MODIS, we used the BRDF model described in Section 2, and derived data from Terra MODIS to predict the reflectance that would be observed by Aqua MODIS bands 1, 2 and 7 (since band 6 of Aqua MODIS has too many non functioning detectors) for a few months following Aqua MODIS's first light (June 28, 2002). The ratio of observed to predicted Aqua MODIS reflectance for bands 1 and 2 is plotted as a function of time in Fig. 7a and b. These



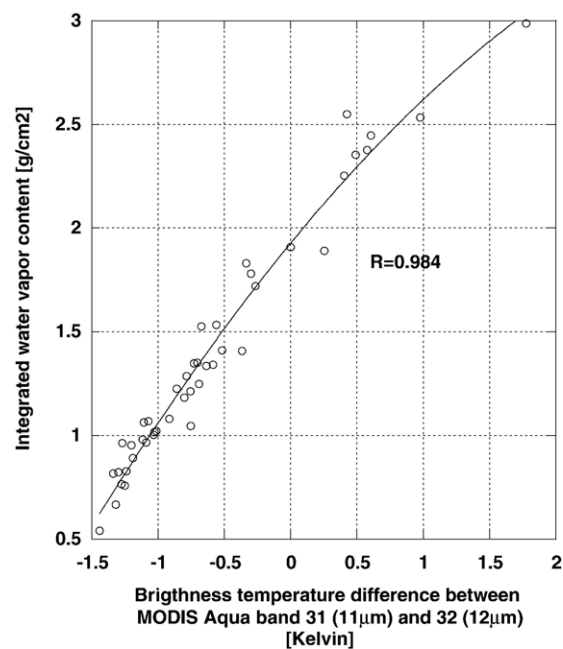
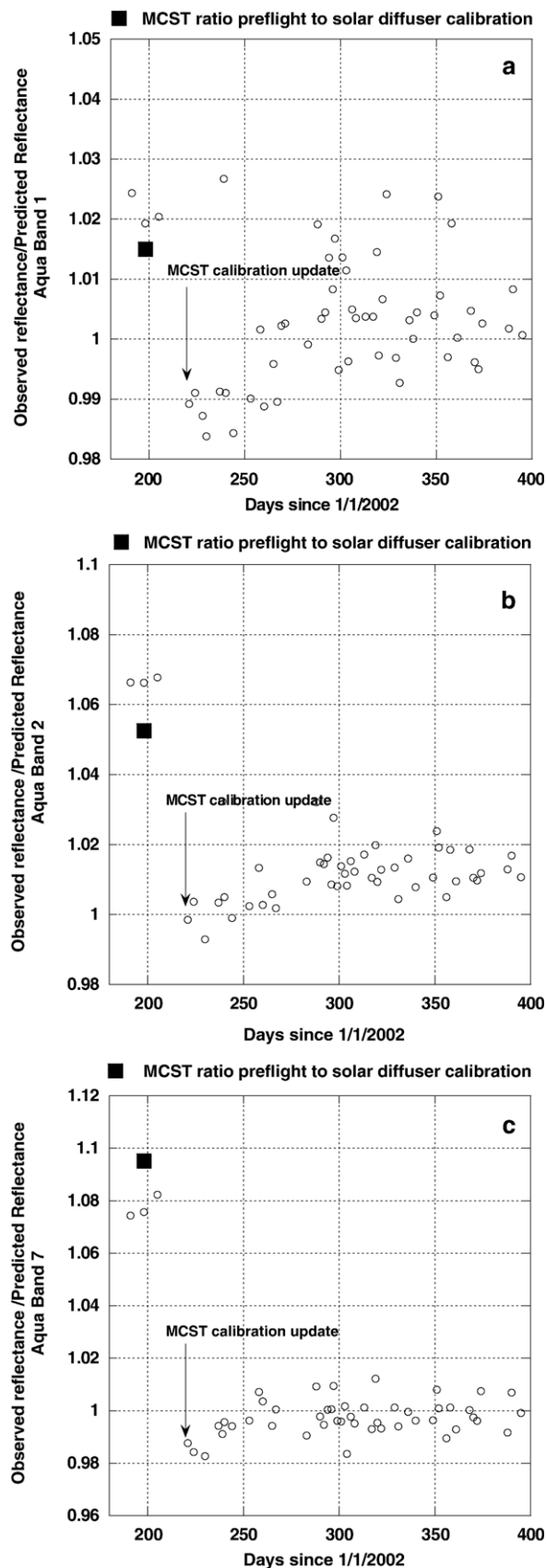


Fig. 8. Integrated water vapor content derived from MODIS near-infrared absorption bands (18 and 19) as a function of brightness temperature difference in bands 31 (11 μm) and 32 (12 μm) for Aqua MODIS data collected over the calibration site from August, 2002 to February, 2003.

figures also show the preflight to in-flight calibration ratio determined by MCST on July 17, 2002 (solid square). We observed modest variations of the predicted-to-retrieved reflectance ratio after the nadir door opened on June 28, 2002. However, the computed observed-to-predicted ratio agrees very well with the preflight-to-in-flight calibration ratio derived by MCST from the solar diffuser on July 17, 2002. The two ratios agree to within 1%. The in-flight calibration derived by MCST on July 17, 2002 started to be used in Aqua MODIS calibration on August 7th, 2002. After that day, the observed-to-predicted reflectance ratio, derived using our cross-calibration approach, fluctuates within 1% around 1.0 for bands 1, 2 and 7, with some occasional outliers within 2%. These results show that the approach can be used to transfer the calibration from Terra MODIS to other sensors using our well characterized calibration site.

#### 4. Application to NOAA16 AVHRR

To apply the cross-calibration approach to AVHRR, onboard NOAA16, we started by deriving the AVHRR surface reflectance over the calibration site using the preflight calibration coefficients. The atmospheric correction approach described in [El Saleous et al. \(2000\)](#) was used to correct for Rayleigh scattering, ozone and water vapor absorption effects. The low spatial resolution of the DAO (Data Assimilation Office) or NCEP

Fig. 7. (a) the ratio between the derived and the predicted Aqua MODIS surface directional reflectance in band 1 (using the Terra derived characteristics of the desert site) for the first 7 months of operation. (b) Same as in (a) but for MODIS band 2. (c) Same as in (a) but for MODIS band 7.

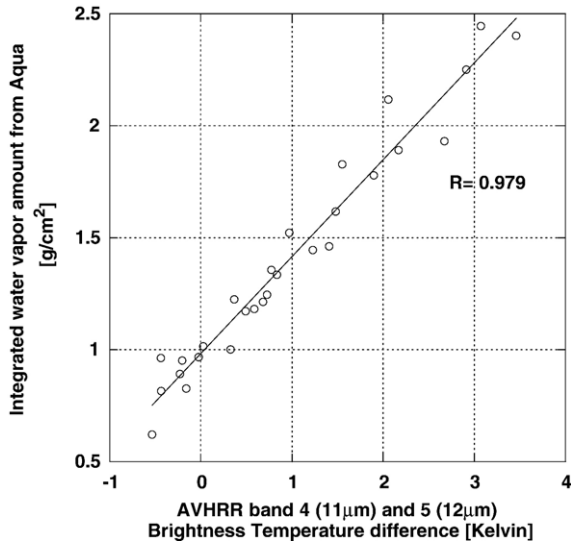


Fig. 9. Integrated water vapor content derived from Aqua MODIS near-infrared absorption bands (18 and 19) as a function of the temperature difference in bands 4 (11 µm) and 5 (12 µm) for AVHRR data collected over the calibration site.

(National Centers for Environmental Prediction) water vapor ancillary data suggested by El Saleous et al. (2000) proved inadequate for use over the calibration site. We adopted a split window technique to derive the integrated water vapor content

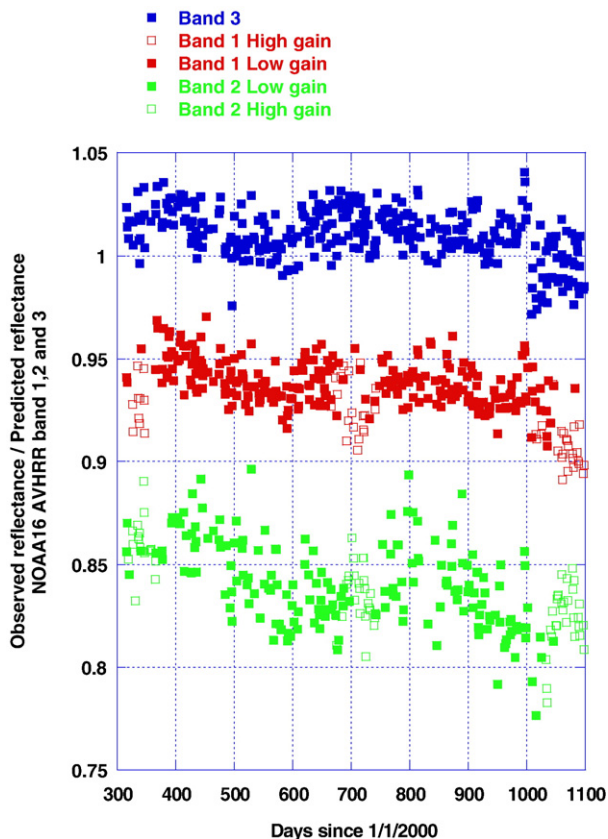


Fig. 10. Variation of the retrieved to predicted surface directional reflectance ratio for NOAA16 AVHRR during the period from November, 2000 to February, 2003.

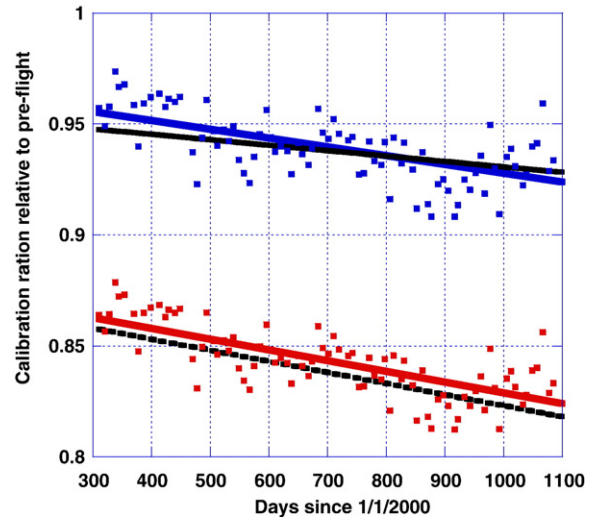


Fig. 11. Comparison of the desert calibration trends for band 1 (black solid line) and band 2 (black interrupted line), with the trends obtained using the Ocean and Clouds method (Vermote and Kaufman, 1995) for band 1 (blue line and square) and band 2 (red line and square).

over the calibration sites using AVHRR bands 4 (11 µm) and 5 (12 µm). The approach relies on correlating the difference in brightness temperature from AVHRR bands 4 and 5 to water vapor content derived from coincident Aqua MODIS data. We first validated this technique using Aqua MODIS by comparing the temperature difference observed in MODIS bands 31 and 32 with the integrated water vapor content derived from the near-infrared MODIS bands 18 and 19 (Gao & Kaufman, 2003). We used data from August 2002 to February 2003, where the calibration in the thermal infrared was very stable, to ensure good retrieval of integrated water vapor content. Fig. 8 shows the comparison between the integrated water vapor content derived from the MODIS near-infrared absorption bands with the temperature difference in the long-wave infrared. The very high correlation observed in Fig. 8 demonstrates the feasibility of the use of long-wave brightness temperature difference to retrieve integrated water vapor content for this site through a linear relationship. To derive the coefficients for NOAA16 AVHRR, the difference in brightness temperature in bands 4 and 5 is plotted against the integrated water vapor content derived from Aqua MODIS near-infrared bands 18 and 19 (Fig. 9). Only Aqua observations that occurred within 30 min of the AVHRR acquisition are used. The water vapor content is highly correlated to the difference in temperature ( $R=0.979$ ) and can be derived using the linear equation:

$$u_{wv}[\text{g/cm}^2] = a\Delta T[K] + b \quad (1)$$

where  $a=0.418$  and  $b=1$ .

In the next step, predicted AVHRR reflectance for bands 1, 2 and 3 were computed using the site model described in Section 2. The BRDF model with the coefficients listed in Table 1 was used to derive a MODIS-like reflectance, which in turn is adjusted to AVHRR bands using the spectral translation coefficients listed in Table 1. The ratios between the observed and the predicted

reflectance for AVHRR bands 1, 2 and 3 are plotted in Fig. 10 as a function of time. Fig. 10 shows that for bands 1 and 3 the dispersion is very small along the general time trend (RMS of 0.008 for band 1 and 0.01 for band 3), while band 2 shows more dispersion (RMS of 0.0145), likely due to residual water vapor effects. NOAA16 AVHRR has a bi-linear gain feature. Over the desert site, observations are always acquired at low gain for band 3, but can be acquired in either low or high gain for bands 1 and 2. Both gains are reported for bands 1 and 2, with no major bias observed by switching gains.

The ratios presented on Fig. 10 are relative to the pre-launch calibration of NOAA16, indicating that the pre-launch calibration of bands 3 and 1 was within 5% of the in-flight values. For band 2 the pre-launch calibration was off by 15%. This is consistent with what has been observed on previous NOAA 7, 9, and 11, where the preflight calibration in band 1 has always been closer to in-flight ( $\pm 5\%$ ) than the one in band 2 (15% or worse). However the reasons for those discrepancies are unknown to us.

We want to recognize that in a general case one will want to simulate the signal observed by AVHRR and compare top of atmosphere values instead of comparing the surface reflectance to the BRDF prediction. We did the latter rather than the former because of practical constraints. In this specific case, the site is of relatively high reflectance, with a solar angle generally varying from 15 to 55°. Therefore, the difference between the two approaches is small. By using extreme geometry (sun at 55°, view at 50°), one can show that the difference between using top of atmosphere versus surface value for determining the degradation is around 0.8% in band 1, 0.6% in band 2 and 0.1% in band 3, which is well beyond the estimated accuracy of MODIS calibration itself.

Finally, the calibration coefficients derived over the desert site by cross-calibration are compared to those derived over ocean and clouds (Vermote & Kaufman, 1995). These coefficients are available from the AVHRR Long Term Data Record website at <http://ltdr.nascom.nasa.gov/ltdr/ltdr.html>. The results derived by the two independent methods are in very good agreement (Fig. 11). The calibration trends are almost the same and absolute values are within 1%, which is well within the expected errors of both methods.

## 5. Conclusions

This study presents an approach to transfer the calibration of reflectance bands from a well calibrated sensor (MODIS) to other sensors (AVHRR) using a desert target. The approach relies on developing an accurate parameterization of the calibration site using a short time series of MODIS data and a widely used BRDF model. Applying this approach to another sensor, with well

defined calibration (Aqua MODIS), shows that the method enables cross-calibration with very good accuracy (1%).

This approach was applied to AVHRR onboard NOAA16 where the vicarious calibration coefficients were derived for bands 1 to 3. The results for bands 1 and 2 were compared to the calibration coefficients derived using the ocean and clouds technique (Vermote & Kaufman, 1995) and were found consistent to within 1%. Validating the results of the ocean and clouds calibration technique is of paramount importance as this approach has been used to apply a consistent calibration to the AVHRR record since 1981 (<http://ltdr.nascom.nasa.gov/ltdr/ltdr.html>) as the first step to creating a long term data set for land and climate studies.

## References

- El Saleous, N. Z., Vermote, E. F., Justice, C. O., Townshend, J. R. G., Tucker, C. J., & Goward, S. N. (2000). Improvements in the global biospheric record from the Advanced Very High Resolution Radiometer (AVHRR). *International Journal of Remote Sensing*, 21(6), 1251–1277.
- Gao, B. C., & Kaufman, Y. J. (2003). Water vapor retrievals using Moderate Resolution Imaging Spectroradiometer (MODIS) near-infrared channels. *Journal of Geophysical Research*, 108(D13), 4389.
- Guenther, B., Xiong, X., Salomonson, V. V., Barnes, W. L., & Young, J. (2002). On-orbit performance of the Earth Observing System Moderate Resolution Imaging Spectroradiometer; first year of data. *Remote Sensing Of Environment*, 83, 16–30.
- Heidinger, A. K., Cao, C., & Sullivan, J. T. (2002). Using Moderate Resolution Imaging Spectrometer (MODIS) to calibrate advanced very high resolution radiometer reflectance channels. *Journal of Geophysical Research*, 107 (D23), 4702.
- Heidinger, A. K., Sullivan, J. T., & Rao, N. (2002). Calibration of visible and near-infrared channels of NOAA-12 AVHRR using time-series of observations over deserts. *International Journal of Remote Sensing*, 24(18), 3635–3649.
- Justice, C. O., Eck, T. F., Tanre, D., & Holben, B. N. (1991). The effect of water-vapor on the normalized difference vegetation index derived for the Sahelian region from NOAA AVHRR data. *International Journal of Remote Sensing*, 12(6), 1165–1187.
- Rao, C. R. N., & Chen, J. (1996). Post-launch calibration of the visible and near-infrared channels of the Advanced Very High Resolution Radiometer on NOAA-14 spacecraft. *International Journal of Remote Sensing*, 17, 2743–2747.
- Schaaf, C. B., Gao, F., Strahler, A. H., Lucht, W., Li, X., Tsang, T., et al. (2002). First operational BRDF, albedo nadir reflectance products from MODIS. *Remote Sensing of Environment*, 83, 135–148.
- Teillet, P. M., Barker, J. L., Markham, B. L., Irish, R. R., Fedosejevs, G., Storey, J. C., (2001). Radiometric cross-calibration of the Landsat-7 ETM+ and Landsat-5 TM sensors based on tandem data sets. *Remote Sensing of Environment*, 79, 39–54.
- Vermote, E. F., & Kaufman, Y. J. (1995). Absolute calibration of AVHRR visible and near infrared channels using ocean and cloud views. *International Journal of Remote Sensing*, 16(13), 2317–2340.
- Vermote, E. F., & Roy, D. P. (2002). Land surface hot-spot observed by MODIS over Central Africa. *International Journal of Remote Sensing*, 11, 2141–2143 Cover Letter.